PHYSICAL REVIEW C VOLUME 40, NUMBER 2 AUGUST 1989

Seniority structure of the cranked shell model wave function and the pairing phase transition

C. S. Wu and J. Y. Zeng
Department of Physics, Peking University, Beijing, China
and Center of Theoretical Physics, China Center of Advanced Science and Technology (World Laboratory), Beijing, China
(Received 16 January 1989)

The accurate solutions to the low-lying eigenstates of the cranked shell model Hamiltonian are obtained by the particle-number-conserving treatment, in which a many-particle configuration truncation is adopted instead of the conventional single-particle level truncation. The variation of the seniority structures of low-lying eigenstates with rotational frequency ω is analyzed. The gap parameter of the yrast band decreases with ω very slowly, though the seniority structure has undergone a great change. It is suggested to use the seniority structure to indicate the possible pairing phase transition from a superconducting state to a normal state. The important blocking effects on the low-lying eigenstates are discussed.

I. INTRODUCTION

In the past several years it was found that in a number of deformed nuclei when the rotational frequency ω exceeds a certain value (e.g., $\hbar\omega \geq 0.38$ MeV for Hf isotopes) the yrast bands and some sidebands show the character of a rigid rotor, i.e., their moments of inertia are almost constant and close to the rigid-body value.[1] This fact seems to imply that the neutron pairing correlation has effectively disappeared at these high rotational frequencies (the Mottelson-Valatin effect[2]). But as pointed out in Ref. 3, the moment of inertia deduced from the energy spectra is of limited value to indicate a pairing phase transition from a superconducting state to a normal state, and the surprisingly constant moments of inertia near rigid-body values are not an indication of a pairing collapse. Indeed, in all self-consistent solutions to the cranked Hartree-Fock-Bogoliubov (HFB) equations a pairing collapse has been found,[4-6] but the results obtained without particle-number projection are not reliable.[3,6] Calculations with particle-number projection before variation show that the gap parameter decreases very slowly and no sharp phase transition is found.

The particle-number-conserving (PNC) approach for treating the pairing Hamiltonian[7,8] is extended to treat the eigenvalue problem of the cranked shell model (CSM) Hamiltonian for well-deformed nuclei. Instead of a single-particle level (SPL) truncation (usually adopted in the shell model calculation, BCS or HFB method, etc.), a many-particle configuration (MPC) truncation is used in the PNC formalism. In this formalism all the many-particle configurations are taken into account provided their configuration energies (i.e., the sums of single-particle energies) are less than a given value, the truncation energy. It was shown[9] that on the one hand, in view of the many-body character of the Hamiltonian, the MPC truncation is more reasonable than the SPL truncation; and on the other hand, the MPC truncation is more effective in practical numerical calculation for the low-lying excited states of a many-particle system. In the usual SPL truncation, while a great number of configurations (which is very unimportant in the low-lying excited states) are involved in the calculation and make the calculation very tedious and time consuming, a large number of configurations (which is relatively important in the low-lying excited states) are omitted and make some results unsatisfactory from the physical point of view. Calculation shows that the number of main configurations (i.e., weight $\geq 1\%$) in the low-lying excited eigenstates is very limited and the energies of all these main configurations are relatively low. Therefore it is not difficult to obtain a sufficiently accurate solution to the low-lying excited eigenstates by diagonalizing the CSM Hamiltonian in a sufficiently large truncated configuration space. All the serious troubles encountered in the BCS or HFB treatment, such as the nonconservation of particle number, the occurrence of excessive spurious states in the low-lying excited spectra, etc., disappear in the PNC approach. Moreover, the important blocking effects are taken into account exactly in the PNC code.

The general formalism of the PNC treatment for the CSM eigenvalue problem is given in Sec. II. Calculations in a single-j model[10,11] and discussions about the seniority structure of the CSM wave functions and the problem of pairing phase transition are given in Sec. III. Calculations can be extended straightforwardly to a more realistic single-particle level scheme, e.g., the Nilsson level scheme, and results will be published subsequently.

II. FORMALISM

A. Hamiltonian

Usually the CSM Hamiltonian of an axially symmetric nucleus in the rotating frame is expressed as

$$H_{\mathrm{CSM}} = H_{\mathrm{intr}} + H_C \ , \tag{1}$$

where H_C is the Coriolis interaction (x denotes the rotating axis which is perpendicular to the symmetry z axis),

$$H_C=-\omega J_x \ , \tag{2}$$

and

$$H_{\text{intr}}=H_{\text{sp}}+H_P \ . \tag{3}$$

H_{SP} is the single-particle Hamiltonian and H_P the pairing interaction. It is convenient to choose a representation in which H_{SP} is diagonal, then

$$H_{\text{SP}}=\sum_{\nu>0}\epsilon_\nu(a_\nu^\dagger a_\nu+a_{\bar\nu}^\dagger a_{\bar\nu}) \ , \tag{4}$$

$$H_P=-GP^\dagger P \ , \tag{5}$$

$$P^\dagger=\sum_{\nu>0}a_\nu^\dagger a_{\bar\nu}^\dagger, \quad P=\sum_{\nu>0}a_{\bar\nu}a_\nu \ , \tag{6}$$

$$H_C=-\omega\sum_{\mu,\nu}\langle\mu|j_x|\nu\rangle a_\mu^\dagger a_\nu \ , \tag{7}$$

where G is the average pairing strength, μ and ν label the single-particle states, $\bar\mu$ and $\bar\nu$ denote the time-reversed states, and ϵ_ν is the twofold degenerate single-particle energy.

B. Single-particle states

When $\omega=0$ the z component of nuclear angular momentu, $J_z=\sum_i(j_z)_i$, is conserved, where $(j_z)_i$ is the z component of angular momentum of the ith nucleon. In this case the single-particle state may be specified by Ω_i (eigenvalue of j_z) and parity π_i, and $K=\sum_i\Omega_i$ is a good quantum number. $H_{\text{CSM}}=H_{\text{intr}}$ may be diagonalized in each subspace with fixed K, parity $\pi=\prod_i\pi_i$, and seniority v (the number of unpaired particles).

However, for $\omega\neq0$, J_z is no longer conserved, and it is not suitable to use Ω to label the single-particle state. Usually, H_{SP} is assumed to be $R_x(\pi)$ invariant, where $R_x(\pi)$ is a rotation of π around the x axis, i.e., $[R_x(\pi),H_{\text{SP}}]=0$, hence $[R_x(\pi),H_{\text{CSM}}]=0$. In this case we may diagonalize the Hamiltonian (1) in each subspace with fixed signature r [eigenvalue of $R_x(\pi)$] and parity π. Therefore it is convenient to use signature $r\ (=\pm i)$ to label the single-particle state. Considering the fact that $[j_z^2,R_x(\pi)]=0$, the eigenstate of $R_x(\pi)$ may be expressed as a linear combination of the twofold degenerate eigenstates of j_z^2. For definiteness, let χ_Ω denote the eigenstate of j_z with $\Omega>0$, and

$$\chi_{\bar\Omega}=R_x(\pi)\chi_\Omega=e^{-i\pi j_x}\chi_\Omega \ , \tag{8}$$

which is also an eigenstate of j_z with eigenvalue $-\Omega$. ($\chi_{\bar\Omega}$ is also the time-reversed state of χ_Ω except for a possible phase factor.) Both χ_Ω and $\chi_{\bar\Omega}$ are the eigenstates of j_z^2 with eigenvalue Ω^2. Define

$$\varphi_{\Omega\alpha}=\frac{1}{\sqrt2}[1+e^{i\pi\alpha}R_x(\pi)]\chi_\Omega=\frac{1}{\sqrt2}(\chi_\Omega+e^{i\pi\alpha}\chi_{\bar\Omega}), \quad \alpha=\tfrac12$$
$$\varphi_{\Omega\bar\alpha}=\frac{1}{\sqrt2}[e^{i\pi\alpha}+R_x(\pi)]\chi_\Omega=\frac{1}{\sqrt2}(e^{i\pi\alpha}\chi_\Omega+\chi_{\bar\Omega}) \ , \tag{9}$$
$$\bar\alpha=-\tfrac12 \ .$$

It is easy to show that

$$R_x(\pi)\varphi_{\Omega\alpha}=e^{-i\pi\alpha}\varphi_{\Omega\alpha}=-i\varphi_{\Omega\alpha} \ ,$$
$$R_x(\pi)\varphi_{\Omega\bar\alpha}=e^{i\pi\alpha}\varphi_{\Omega\bar\alpha}=+i\varphi_{\Omega\bar\alpha} \ . \tag{10}$$

In the second quantization formalism the canonical transformation (9) can be expressed as

$$b_\nu^\dagger=\frac{1}{\sqrt2}(a_\nu^\dagger+e^{i\pi\alpha}a_{\bar\nu}^\dagger) \ ,$$
$$b_{\bar\nu}^\dagger=\frac{1}{\sqrt2}(e^{i\pi\alpha}a_\nu^\dagger+a_{\bar\nu}^\dagger) \ . \tag{11}$$

It can be verified that

$$\{b_\nu,b_{\nu'}^\dagger\}=\delta_{\nu\nu'} \ ,$$
$$\{b_{\bar\nu},b_{\bar\nu'}^\dagger\}=\delta_{\nu\nu'} \ , \tag{12}$$

other anticommutators vanish, and the form of the pair-creation operator remains unchanged under this transformation, namely, $a_\nu^\dagger a_{\bar\nu}^\dagger=b_\nu^\dagger b_{\bar\nu}^\dagger$. In the new representation the matrix elements of the single-particle angular momentum j_x can be evaluated as follows.

(a) The matrix element of j_x between two single-particle states of opposite signature vanishes:

$$\langle\varphi_{\Omega_1\alpha}|j_x|\varphi_{\Omega_2\bar\alpha}\rangle=0 \ . \tag{13}$$

(b) The matrix element of J_x between two single-particle states of the same signature is

$$\langle\varphi_{\Omega_1\alpha}|j_x|\varphi_{\Omega_2\alpha}\rangle$$
$$=\langle\chi_{\Omega_1}|j_x|\chi_{\Omega_2}\rangle+e^{-i\pi\alpha}\langle\chi_{\bar\Omega_1}|j_x|\chi_{\Omega_2}\rangle\delta_{\Omega_1,1/2}\delta_{\Omega_2,1/2} \ , \quad \alpha=\pm\tfrac12 \tag{14}$$

where $\langle\chi_{\Omega_1}|j_x|\chi_{\Omega_2}\rangle$ and $\langle\chi_{\bar\Omega_1}|j_x|\chi_{\Omega_2}\rangle$ can be calculated in a Nilsson state basis.

(c) In particular, the matrix element for $\Omega_1=\Omega_2=\frac12$ is

$$\langle\varphi_{\Omega_1\alpha}|j_x|\varphi_{\Omega_2\alpha}\rangle=e^{-i\pi\alpha}\langle\chi_{\bar\Omega_1}|j_x|\chi_{\Omega_2}\rangle \ , \tag{15}$$

which is the only type of matrix element depending on the signature and is responsible for all the signature splitting.

C. Many-particle configurations

For the ground band and the related low-lying excited bands of a $2n$-particle system the configurations needed to be considered are those of signature $r=+$ and parity $\pi=+$, which can be constructed as follows.

(a) The fully paired configuration ($v=0$):

$$|\rho_1\bar\rho_1\rho_2\bar\rho_2\cdots\rho_n\bar\rho_n\rangle=b_{\rho_1}^\dagger b_{\bar\rho_1}^\dagger b_{\rho_2}^\dagger b_{\bar\rho_2}^\dagger\cdots b_{\rho_n}^\dagger b_{\bar\rho_n}^\dagger|0\rangle \ ,$$
$$K\pi=0+ \ . \tag{16}$$

(b) Configurations with two unpaired particles ($v=2$):

$$|\nu_1\bar\nu_2\rho_1\bar\rho_1\cdots\rho_{n-1}\bar\rho_{n-1}\rangle$$
$$=b_{\nu_1}^\dagger b_{\bar\nu_2}^\dagger b_{\rho_1}^\dagger b_{\bar\rho_1}^\dagger\cdots b_{\rho_{n-1}}^\dagger b_{\bar\rho_{n-1}}^\dagger|0\rangle \ , \tag{17}$$
$$\pi_{\nu_1}=\pi_{\nu_2}, \quad K=\pm|\Omega_{\nu_1}-\Omega_{\nu_2}|,\pm(\Omega_{\nu_1}+\Omega_{\nu_2}) \ .$$

For a given pair of single-particle levels occupied by unpaired particles there are two different combinations with $\alpha=0$, i.e., $(\nu_1,\bar{\nu}_2)$ and $(\nu_2,\bar{\nu}_1)$. Both of them have to be considered simultaneously.

(c) Configurations with four unpaired particles ($v=4$):

$$|\nu_1\nu_2\bar{\nu}_3\bar{\nu}_4\rho_1\bar{\rho}_1\cdots\rho_{n-2}\bar{\rho}_{n-2}\rangle = b^\dagger_{\nu_1}b^\dagger_{\nu_2}b^\dagger_{\bar{\nu}_3}b^\dagger_{\bar{\nu}_4}b^\dagger_{\rho_1}b^\dagger_{\bar{\rho}_1}\cdots b^\dagger_{\rho_{n-2}}b^\dagger_{\bar{\rho}_{n-2}}|0\rangle\ , \quad (18)$$

$$\pi_{\nu_1}\pi_{\nu_2}\pi_{\nu_3}\pi_{\nu_4}=+\ .$$

For given two pairs of single-particle level occupied by unpaired particles, e.g., 1, 2, 3, and 4, there are 8 combinations of $r=(e^{-i\pi\alpha})=1$. Six of them are of $\alpha=0$, namely,

$$|12\bar{3}\bar{4}\rangle,|13\bar{2}\bar{4}\rangle,|14\bar{2}\bar{3}\rangle,|23\bar{1}\bar{4}\rangle,|24\bar{1}\bar{3}\rangle,|34\bar{1}\bar{2}\rangle \quad (19)$$

and the other two

$$|1234\rangle \text{ and } |\bar{1}\bar{2}\bar{3}\bar{4}\rangle \quad (20)$$

are of $\alpha=\pm2$.

(d) Configurations with six or more unpaired particles ($v\geq6$) can be written out similarly. However, calculations show that for not too high rotational frequency the contribution of configurations with $v\geq6$ to the yrast and the low-lying excited bands is negligibly small.

As mentioned above, the single-particle Hamiltonian $H_{\rm SP}$ is diagonal with respect to this configuration space. The matrix elements of H_P between many-particle configurations are (a) diagonal element: $-G\times$ (number of particles pairs), (b) off-diagonal element: $-G$, if two configurations differ by one particle pair; 0, otherwise.

The matrix elements of H_C (or J_x) between many-particle configurations are given in the Appendix. The related selection rules are as follows.

a. The angular momentum selection rule, $\Delta K=\pm1$. Hence the matrix elements of H_C between fully paired configurations ($v=0$, $K\pi=0+$) vanish.

b. The seniority selection rule, $\Delta v=0,\pm2$. Because H_C is a one-body operator, a vanishing matrix element will be expected between two configurations which differ by more than one single-particle state.

c. The signature selection rule, $\Delta\alpha=0$. This selection rule originates from the $R_x(\pi)$ invariance and the one-body character of H_C. It should be noted that the α-selection rule ($\Delta\alpha=0$) is stronger than the r-selection rule (Δr, *no*). Configurations with the same r but different α cannot be mixed with each other. For example, the configurations with $\alpha=0$ in Eq. (19) cannot mix with those with $\alpha=\pm2$ in Eq. (20).

D. General form of the eigenstates of the CSM Hamiltonian

Take a $2n$-particle system as an example. The eigenstates of parity $\pi=+$ and $\alpha=0$ are expressed as

$$|2n,\beta,\pi=+,\alpha=0\rangle=\sum_{\rho_1,\cdots,\rho_n}V^{\beta}_{\rho_1\cdots\rho_n}|\rho_1\bar{\rho}_1\cdots\rho_n\bar{\rho}_n\rangle+\sum_{\nu_1,\nu_2}\sum_{\rho_1,\cdots,\rho_{n-1}}V^{\beta(\nu_1\nu_2)}_{\rho_1\cdots\rho_{n-1}}|\nu_1\bar{\nu}_2\rho_1\bar{\rho}_1\cdots\rho_{n-1}\bar{\rho}_{n-1}\rangle\ ,$$
$$+\sum_{\nu_1,\nu_2,\nu_3,\nu_4}\sum_{\rho_1,\cdots,\rho_{n-2}}V^{\beta(\nu_1\nu_2\nu_3\nu_4)}_{\rho_1\cdots\rho_{n-2}}|\nu_1\nu_2\bar{\nu}_3\bar{\nu}_4\rho_1\bar{\rho}_1\cdots\rho_{n-2}\bar{\rho}_{n-2}\rangle+\cdots\ ,$$
$$\beta=0\ (\text{yrast}),\quad 1,2,3,\ldots\ (\text{excited states})\ . \quad (21)$$

By diagonalizing $H_{\rm CSM}$ in a sufficiently large configuration space, $(E-E_0)\leq E_c$, we can obtain sufficiently accurate solutions to the yrast states and the low-lying excited eigenstates, and then we can extract all the desired information on these eigenstates. For example, the seniority structure P_v (the component of the configurations with seniority v) can be calculated as follows:

$$P_0^{(\beta)}=\sum_{\rho_1,\cdots,\rho_n}|V^{\beta}_{\rho_1\cdots\rho_n}|^2\ ,$$
$$P_2^{(\beta)}=\sum_{\nu_1,\nu_2}\sum_{\rho_1,\cdots,\rho_{n-1}}|V^{\beta(\nu_1\nu_2)}_{\rho_1\cdots\rho_{n-1}}|^2\ , \quad (22)$$
$$P_4^{(\beta)}=\sum_{\nu_1,\nu_2,\nu_3,\nu_4}\sum_{\rho_1,\cdots,\rho_{n-2}}|V^{\beta(\nu_1\nu_2\nu_3\nu_4)}_{\rho_1\cdots\rho_{n-2}}|^2$$
$$\cdots\ .$$

where P_v's are constrained by the normalization condition

$$P_0^{(\beta)}+P_2^{(\beta)}+P_4^{(\beta)}+\cdots=1\ . \quad (23)$$

E. Nuclear pairing phase transition

The most direct evidence for a pairing phase transition should be given by the pair-transfer matrix elements between neighboring even-even nuclei

$$\langle 2n+2,\beta'+0|P^{\dagger}|2n,\beta+0\rangle=\sum_{\mu\rho_1,\ldots,\rho_n} V^{\beta'}_{\mu\rho_1\cdots\rho_n}V^{\beta}_{\rho_1\cdots\rho_n}+\sum_{\nu_1,\nu_2}\sum_{\mu\rho_1,\ldots,\rho_{n-1}} V^{\beta'(\nu_1\nu_2)}_{\mu\rho_1\cdots\rho_{n-1}}V^{\beta(\nu_1\nu_2)}_{\rho_1\cdots\rho_{n-1}}$$
$$+\sum_{\nu_1,\nu_2,\nu_3,\nu_4}\sum_{\mu\rho_1,\ldots,\rho_{n-2}} V^{\beta'(\nu_1\nu_2\nu_3\nu_4)}_{\mu\rho_1\cdots\rho_{n-2}}V^{\beta(\nu_1\nu_2\nu_3\nu_4)}_{\rho_1\cdots\rho_{n-2}}+\cdots . \tag{24}$$

However, it is very difficult so far to measure them at high spins. Another useful quantity is the pairing parameter[12]

$$\tilde{\Delta}=G(\langle P^{\dagger}P\rangle)^{1/2} \tag{25}$$

which coincides with the usual gap parameter Δ in the BCS or HFB theory

$$\Delta=G\langle P\rangle . \tag{26}$$

In Eq. (25) the averaging should be done with respect to the active particle pairs.

III. CALCULATED RESULTS AND DISCUSSIONS

As an illustrative example calculations in a single-j model[10,11]

$$\epsilon_{|\Omega|}=\kappa\frac{3\Omega^2-j(j+1)}{j(j+1)}+e_0,\quad |\Omega|=\tfrac{1}{2},\tfrac{3}{2},\ldots,j \tag{27}$$

are carried out to examine the features of low-lying excited eigenstates. By choosing $e_0=6.655\hbar\omega$, $\kappa=0.392\hbar\omega$, and $j=\frac{13}{2}$ the Nilsson neutron levels at the deformation $\epsilon_2=0.27$ and $\epsilon_4=0.02$, corresponding roughly to the ground state deformation of ^{168}Er, are reproduced within 0.1%.[11] This gives a certain realism to the model. In the single-j model the number of particles $N\leq 2j+1=14$. In the new single-particle basis [Eqs. (9) or (11)], the 14 states are divided into two groups, characterized by the signature, $\alpha=\frac{1}{2}$ and $\alpha=-\frac{1}{2}$, and are denoted by 1,2,3,4,5,6,7 and $\bar{1},\bar{2},\bar{3},\bar{4},\bar{5},\bar{6},\bar{7}$, respectively. To diagonalize $H_{\rm CSM}$ all the many-particle configurations below $E_c=3.5\kappa$ are taken into account. (Calculation within a larger truncated configuration space, $E_c=4.5\kappa$, was also carried out and almost the same low-lying spectra were obtained provided the renormalization of the pairing strength G was considered.) The dimensions of the truncated configuration spaces are

N	2	4	6	8	10	12
$D(N)$	43	204	273	182	84	27

Calculations with several values of G ($G/\kappa=0.10$, 0.15, and 0.20) were done and only the results for $G/\kappa=0.15$ are given in the following.

The low-lying excited spectra of the six-particle system relative to the yrast state, $(E-E_{\rm yrast})/\kappa$, are shown in Fig. 1. The amplitudes of the configurations which seem non-negligible (weight $\geq 0.1\%$) in the yrast state and the yrare state for the six-particle system at $\omega/\kappa=0.10$ are given in Table I. It can be seen that the number of the main configurations (weight $>1\%$) in the low-lying states (specified by * in Table I) is very limited (<20) and is much smaller than the dimensions of the truncated configuration space. Also it is seen that all the energies of the main configurations are smaller than 2.0κ. Calculations with even larger truncated configuration spaces show that all the configurations with weight $\geq 0.1\%$ lie below $E/\kappa=3.5$. Therefore the CSM solutions thus obtained to the low-lying excited states are accurate enough and reliable. Thus we can understand why a larger truncated configuration space will yield almost the same low-lying excitation spectra provided the renormalization of G is considered.

From Fig. 1 it is seen that the first bandcrossing occurs at $\omega=\omega_c$ ($\omega_c/\kappa\approx 0.121$), where $\langle J_x\rangle_{\rm yrast}-\langle J_x\rangle_{\rm yrare}=0$. The ω variations of the seniority structure of the yrast state, the first (yrare) and the third excited states are shown in Fig. 2. At $\omega=0$ the yrast state is a coherent superposition of fully paired configurations [$P_0=1$, see Fig. 2(a)]. With increasing ω, the components of seniority $v=2$ and 4 are mixed gradually into the yrast state. It can be seen that for $\omega\geq\omega_c$ the seniority structure of the yrast state has undergone a great change, the component of fully paired configurations, P_0, decreases below 50%, the component of one-pair-broken configurations, P_2, increases up to 40%, and P_4 becomes non-negligible ($\approx 10\%$), while P_6 is still negligibly small.

The yrare state (No. 1 in Fig. 1) at $\omega=0$ is a superposition of broken-pair ($v=2$) configurations with blocked

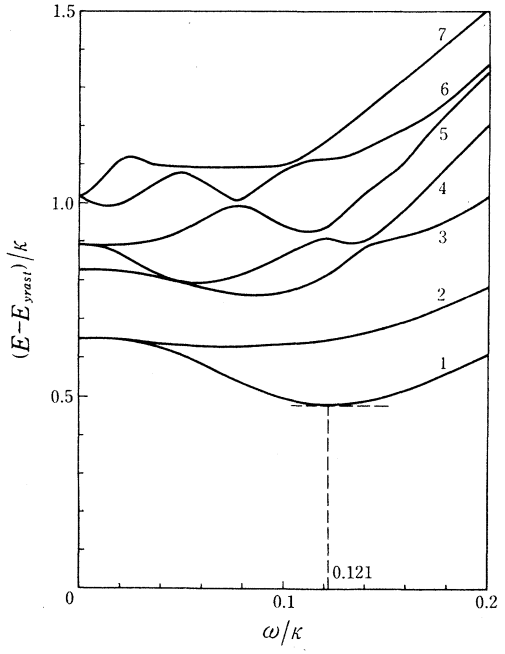

FIG. 1. The low-lying excitation spectra of a six-particle system in the single-j CSM (yrast reference). $E_c/\kappa=3.5$, $G/\kappa=0.15$.

TABLE I. The non-negligible configurations (weight $>0.1\%$) in the low-lying excited states of the six-particle system at $\omega/\kappa=0.10$. The first and the second columns list the configurations and the corresponding energies (in unit κ). The third and the fourth columns list the amplitudes of the non-negligible configurations in the yrast and the yrare bands, respectively. The main configurations with weight $\geq 1\%$ are specified by *. In the first column, 123 means that the single-particle levels 1, 2, and 3 are each occupied by one pair of particles. $(3\bar{4})12$ represents a pair-broken configuration, in which the unpaired particles block the single-particle states 3 and $\bar{4}$ and the remaining two pairs of particles occupy the single-particle levels 1 and 2. $(23\bar{4}\,\bar{5})1$ denotes a $v=4$ configuration, in which the unpaired particles block the single-particle states 2, 3, $\bar{4}$, and $\bar{5}$ and the remaining one pair of particles occupy the single-particle level 1, etc.

Configurations	Configuration energies (κ)	Amplitudes in yrast state	Amplitudes in yrare state
123	0	*0.5492	*−0.3512
124	0.7385	*0.3972	
125	1.7231	*0.1256	
126	2.9538	0.0517	
134	1.2308	*0.2112	0.0958
135	2.2154	0.0985	
136	3.4461	0.0378	
145	2.9538	0.0443	
234	1.4769	*0.1235	
235	2.4615	0.0658	
245	3.2000	0.0381	
$(3\bar{4})12$	0.3692	*0.3219	
$(3\bar{4})15$	2.5846	0.0326	
$(4\bar{3})12$	0.3692	*0.3165	*−0.2640
$(4\bar{3})15$	2.5846	0.0322	
$(2\bar{4})13$	0.6154	*−0.1464	*−0.3153
$(4\bar{2})13$	0.6154	*−0.1301	*0.1259
$(1\bar{4})23$	0.7385	0.0747	*0.4171
$(4\bar{1})23$	0.7385	0.0331	−0.0346
$(3\bar{5})12$	0.8615	0.0899	0.0862
$(5\bar{3})12$	0.8615	0.0870	−0.0838
$(2\bar{3})14$	0.9846	*0.1846	*0.2522
$(2\bar{3})15$	1.9692	0.0577	0.0647
$(3\bar{2})14$	0.9846	*0.1702	
$(3\bar{2})15$	1.9692	0.0537	
$(1\bar{3})24$	1.1077	−0.0929	*−0.3489
$(1\bar{3})25$	2.0923		0.0915
$(3\bar{1})24$	1.1077	−0.0466	
$(2\bar{5})13$	1.1077	−0.0606	*−0.2108
$(2\bar{5})14$	1.8462		−0.0668
$(5\bar{2})13$	1.1077	−0.0516	0.0533
$(1\bar{5})23$	1.2308	0.0369	*0.2593
$(1\bar{5})24$	1.9692		0.0915
$(4\bar{5})12$	1.2308	*0.1180	−0.0684
$(4\bar{5})13$	1.7231	0.0716	0.0771
$(4\bar{5})23$	1.9692	0.0382	
$(5\bar{4})12$	1.2308	*0.1169	
$(5\bar{4})13$	1.7231	0.0708	0.0451
$(5\bar{4})23$	1.9692	0.0379	
$(1\bar{2})34$	1.3538	0.0973	*0.1585
$(1\bar{2})35$	2.3385	0.0415	0.0484
$(2\bar{1})34$	1.3538	0.0591	
$(2\bar{6})13$	1.7231		−0.0500
$(1\bar{6})23$	1.8462		0.0595
$(23\bar{4}\,\bar{5})1$	1.4769		−0.0622
$(24\bar{3}\,\bar{5})1$	1.4769	−0.0715	*−0.1554
$(25\bar{3}\,\bar{4})1$	1.4769	−0.0595	−0.0746
$(34\bar{2}\,\bar{5})1$	1.4769	−0.0553	
$(45\bar{2}\,\bar{3})1$	1.4769	−0.0642	

TABLE I. (*Continued*).

Configurations	Configuration energies (κ)	Amplitudes in yrast state	Amplitudes in yrare state
$(13\bar{4}\,\bar{5})2$	1.6000		0.0839
$(14\bar{3}\,\bar{5})2$	1.6000	0.0408	*0.1924
$(15\bar{3}\,\bar{4})2$	1.6000		*0.1027
$(14\bar{2}\,\bar{5})3$	1.8462	−0.0390	−0.0898
$(15\bar{2}\,\bar{4})3$	1.8462	−0.0372	−0.0621
$(24\bar{3}\,\bar{6})1$	2.0923		−0.0361
$(13\bar{2}\,\bar{5})4$	2.2154		0.0352
$(14\bar{3}\,\bar{6})2$	2.2154		0.0425

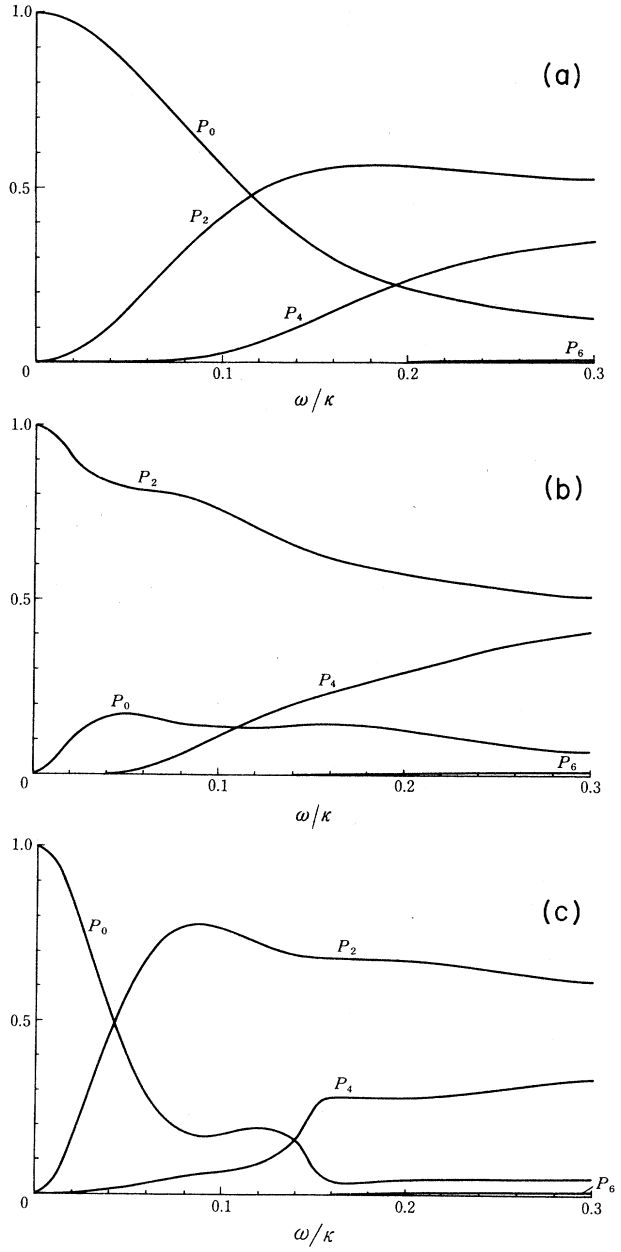

FIG. 2. The ω variation of the seniority structure of a six-particle system. P_v is the weight of the configurations with seniority v ($v=0$, 2, 4, and 6). (a) Yrast band. (b) The first excitation band. (c) The third excitation band.

single-particle levels No. 3 ($|\Omega|=\frac{5}{2}$) and No. 4 ($|\Omega|=\frac{7}{2}$) and $|K|^{\pi}=1^{+},6^{+}$. With increasing ω the component of seniority $v=0$ and 4 are mixed into the yrare states gradually. For $\omega/\kappa>0.20$ the dominant components are of $v=2$ and 4.

At $\omega=0$ the third excited state (No. 3 in Fig. 1) is a pair-excited state ($v=0$, $K^{\pi}=0^{+}$) orthogonal to the yrast state. Its seniority structure changes drastically with increasing ω due to mixture with the other excited states distributed densely in its neighborhood.

The dashed curve in Fig. 3 represents the $\tilde{\Delta}/\tilde{\Delta}(\omega=0)$ averaged over the yrast states of six- and eight-particle systems. It is seen that the calculated pairing parameter $\tilde{\Delta}$ for the yrast state decreases very slowly with ω, similar to the result obtained in Ref. 3 by the HFB calculation with particle-number projection before variation. It is worthwhile to note that $\tilde{\Delta}$ still remains rather large although the seniority structure of the CSM wave function has undergone a great change. Therefore it seems unreasonable to use $\tilde{\Delta}$ to indicate a possible pairing phase transition.

The results for pair-transfer strength between the yrast states of six- and eight-particle systems are shown by the dotted curve in Fig. 3. R value is defined by

$$R=\frac{|\langle 2n+2,\beta=0,+0|P^{\dagger}|2n,\beta=0,+0\rangle|^2}{|\langle 2n+2,\beta=0,+0|P^{\dagger}|2n,\beta=0,+0\rangle|^2_{(\omega=0)}}\,. \tag{28}$$

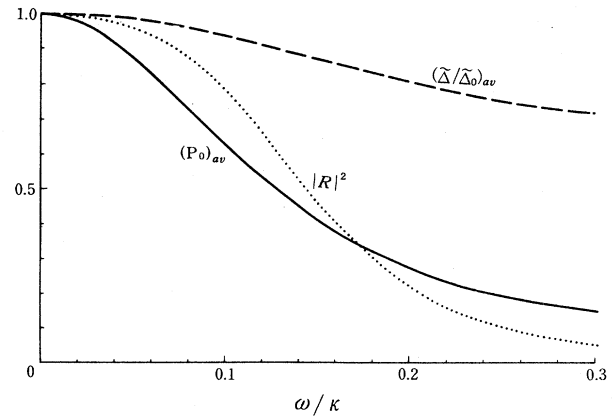

FIG. 3. The dotted line shows the ω variation of the pair-transfer strength between the yrast bands of the six- and eight-particle systems. The dashed line represents the value of $\tilde{\Delta}/\tilde{\Delta}_{(\omega=0)}$, averaged over the yrast bands of the six- and eight-particle systems. The solid line gives the P_0 value averaged over the yrast bands of the six- and eight-particle systems.

The $(P_0)_{av}$ value (solid line in Fig. 3) is the component of fully paired configurations for the yrast states averaged over six- and eight-particle systems. The variation of $(P_0)_{av}$ with ω is similar to that of R. However, both R and $(P_0)_{av}$ decrease with increasing ω faster than $\tilde{\Delta}$ does. Therefore it seems more reasonable to use P_0, the component of fully paired configurations, to indicate a possible pairing phase transition in rotating deformed nuclei.

Finally, the $\tilde{\Delta}$ values for the first and the second excited bands of the the six-particle system is shown in Fig. 4. It is seen that they are much smaller than that of the yrast band and change only a little with increasing ω. The blocking effect, which is strictly taken into account in our PNC code, plays an essential role for reducing the value of $\tilde{\Delta}$ for the excited bands. As pointed out in Ref. 8 the blocking effect may be considered as another kind of antipairing effect which is very important for the low-lying excited spectra, especially when ω is not too high. But as emphasized by Rowe,[13] while the blocking effects are straightforward it is very difficult to treat them in the BCS or HFB formalism because different quasiparticle bases are introduced for different blocked levels.

IV. SUMMARY

Instead of the usual SPL (single-particle level) truncation the MPC (many-particle configuration) truncation is adopted in our particle-number-conserving treatment for the eigenvalue problem of the CSM Hamiltonian and the very accurate solutions to the low-lying eigenstates are obtained. All the configurations with weight larger than 0.1% in the low-lying eigenstates have been included in the calculation. The troubles encountered in the usual HFB treatment, e.g., the particle-number nonconservation, the occurrence of excessive spurious states, the odd behavior of the cranked HFB solution around the band-crossing, etc. disappear in our calculated results. Thus the information of the low-lying CSM eigenstates extracted from our calculation seems reliable.

Calculation shows that the gap parameter $\tilde{\Delta}=G(\langle P^{\dagger}P\rangle)^{1/2}$ for the yrast band decreases very slowly with increasing ω and no sharp pairing phase transition is found. The ω variation of the seniority structure is analyzed, which is found to be similar to the behavior of pair-transfer strength between neighboring even-N systems. It is suggested to use the seniority structure P_0, i.e., the component of the fully paired configurations in the yrast band, to indicate the possible pairing phase transition. Calculation for a more realistic single-particle level scheme shows that the conclusions drawn above still hold qualitatively. Information about the yrast-yrare interaction strength, the ω variation of K structure (triaxiality) of the low-lying eigenstates, etc. are also obtained and will be published subsequently.

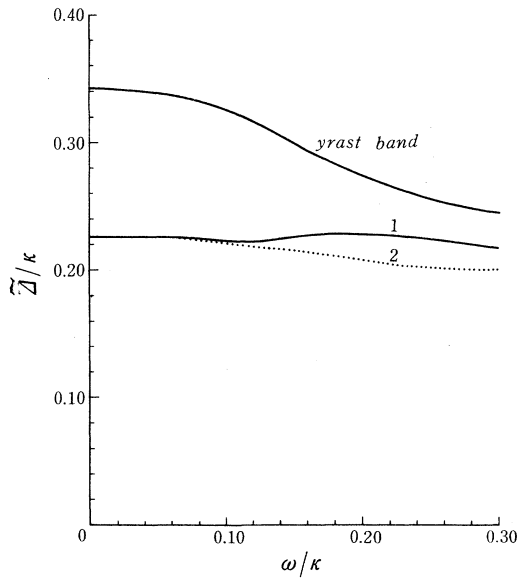

FIG. 4. The ω variation of $\tilde{\Delta}$ values for the yrast band, the first and the second excitation bands of a six-particle system.

The authors would like to express their sincere thanks to Dr. R. Bengtsson, Dr. S. Åberg, and Prof. J. Wood for valuable discussions and comments.

APPENDIX: EVALUATION OF THE MATRIX ELEMENTS OF J_x (OR H_c)

(a) The matrix elements of J_x between fully paired configurations ($v=0$) vanish,

$$\langle\bar{\rho}_{n'}\rho_{n'}\cdots\bar{\rho}_{1'}\rho_{1'}|J_x|\rho_1\bar{\rho}_1\cdots\rho_n\bar{\rho}_n\rangle=0\ . \tag{A1}$$

(b) The matrix element of J_x between a $v=0$ configuration and a $v=2$ configuration may be nonzero only if two configurations differ by one single-particle state, namely,

$$\begin{aligned}\langle\bar{\rho}_{n-1}\rho_{n-1}\cdots\bar{\rho}_1\rho_1\bar{\nu}'\nu|J_x|\mu\bar{\mu}\rho_1\bar{\rho}_1\cdots\rho_{n-1}\bar{\rho}_{n-1}\rangle&\\ \equiv\langle\cdots\bar{\nu}'\nu|J_x|\mu\bar{\mu}\cdots\rangle&\\ \equiv\langle\bar{\nu}'\nu|J_x|\mu\bar{\mu}\rangle&\\ =(j_x)_{\nu\nu'}(\delta_{\mu\nu}+\delta_{\mu\nu'})&\\ +e^{-i\pi\alpha}(j_x)_{\bar{\nu}\nu'}\delta_{\Omega_\nu 1/2}\delta_{\Omega_{\nu'}1/2}(\delta_{\mu\nu}-\delta_{\mu\nu'})\ ,&\end{aligned} \tag{A2}$$

where

$$\begin{aligned}(j_x)_{\nu\nu'}&\equiv\langle\chi_{\Omega_\nu}|j_x|\chi_{\Omega_{\nu'}}\rangle\ ,\\ (j_x)_{\bar{\nu}\nu'}&\equiv\langle\chi_{\bar{\Omega}_\nu}|j_x|\chi_{\Omega_{\nu'}}\rangle\ .\end{aligned} \tag{A3}$$

It should be emphasized that the second term on the right-hand side of Eq. (A2) may not vanish only if $\Omega_\nu=\Omega_{\nu'}=\frac{1}{2}$ and $\pi_\nu=\pi_{\nu'}$.

(c) The matrix elements between $v=2$ configurations. Diagonal element:

$$\langle\cdots\bar{2}1|J_x|1\bar{2}\cdots\rangle=(j_x)_{11}+(j_x)_{\bar{2}\bar{2}}\ . \tag{A4}$$

Off-diagonal element:

$$\langle \cdots \bar{2}'1|J_x|1\bar{2}\cdots\rangle=(j_x)_{\bar{2}'\bar{2}}\ , \tag{A5}$$

$$\langle \cdots \bar{2}1'|J_x|1\bar{2}\cdots\rangle=(j_x)_{1'1}\ , \tag{A6}$$

$$\langle \cdots \bar{2}\bar{2}'1|J_x|1\bar{2}'\bar{2}'\cdots\rangle=-(j_x)_{22'}\ , \tag{A7}$$

$$\langle \cdots \bar{1}\bar{2}1'|J_x|1\bar{2}1'\bar{1}'\cdots\rangle=-(j_x)_{\bar{1}\bar{1}'}\ . \tag{A8}$$

(d) The matrix element between a $v=2$ configuration and a $v=4$ configuration:

$$\langle \cdots \bar{4}\bar{3}21|j_x|1\bar{3}\rho\bar{\rho}\cdots\rangle=-(j_x)_{42}(\delta_{\rho 2}+\delta_{\rho 4})\ , \tag{A9}$$

$$\langle \cdots \bar{4}\bar{3}21|j_x|1\bar{4}\rho\bar{\rho}\cdots\rangle=(j_x)_{32}(\delta_{\rho 2}+\delta_{\rho 3})\ , \tag{A10}$$

$$\langle \cdots \bar{4}\bar{3}21|j_x|2\bar{3}\rho\bar{\rho}\cdots\rangle=(j_x)_{41}(\delta_{\rho 1}+\delta_{\rho 4})\ , \tag{A11}$$

$$\langle \cdots \bar{4}\bar{3}21|j_x|2\bar{4}\rho\bar{\rho}\cdots\rangle=-(j_x)_{31}(\delta_{\rho 1}+\delta_{\rho 3})\ . \tag{A12}$$

(e) The matrix elements between $v=4$ configurations. In view of the signature selection rule ($\Delta\alpha=0$), only the six types of $v=4$ configurations [$\alpha=0$, shown in Eq. (19)] need to be considered for the low-lying eigenstates of an even-N system.

Diagonal element:

$$\langle \cdots \bar{4}\bar{3}21|J_x|12\bar{3}\bar{4}\cdots\rangle = (j_x)_{11}+(j_x)_{22}+(J_x)_{\bar{3}\bar{3}}+(j_x)_{\bar{4}\bar{4}}\ . \tag{A13}$$

Off-diagonal element:

$$\langle \cdots \bar{4}\bar{3}21'|j_x|12\bar{3}\bar{4}\cdots\rangle=(j_x)_{1'1}\ , \tag{A14}$$

$$\langle \cdots \bar{4}\bar{3}2'1|j_x|12\bar{3}\bar{4}\cdots\rangle=(j_x)_{2'2}\ , \tag{A15}$$

$$\langle \cdots \bar{4}\bar{3}'21|j_x|12\bar{3}\bar{4}\cdots\rangle=(j_x)_{\bar{3}'\bar{3}}\ , \tag{A16}$$

$$\langle \cdots \bar{4}'\bar{3}21|j_x|12\bar{3}\bar{4}\cdots\rangle=(j_x)_{\bar{4}'\bar{4}}\ , \tag{A17}$$

$$\langle \cdots \bar{1}\bar{4}\bar{3}21'|j_x|12\bar{3}\bar{4}1'\bar{1}'\cdots\rangle=-(j_x)_{\bar{1}\bar{1}'}\ , \tag{A18}$$

$$\langle \cdots \bar{2}\bar{4}\bar{3}2'1|j_x|12\bar{3}\bar{4}2'\bar{2}'\cdots\rangle=-(j_x)_{\bar{2}\bar{2}'}\ , \tag{A19}$$

$$\langle \cdots \bar{3}\bar{4}\bar{3}'21|j_x|12\bar{3}\bar{4}3'\bar{3}'\cdots\rangle=-(j_x)_{33'}\ , \tag{A20}$$

$$\langle \cdots \bar{4}\bar{4}'\bar{3}21|j_x|12\bar{3}\bar{4}4'\bar{4}'\cdots\rangle=-(j_x)_{44'}\ . \tag{A21}$$

The matrix elements involving $v>4$ configurations may be treated similarly.

[1] R. Chapman *et al.*, Phys. Rev. Lett. **51**, 2265 (1985).
[2] B. R. Mottelson and J. G. Valatin, Phys. Rev. Lett. **5**, 501 (1960).
[3] L. F. Canto, P. Ring, and J. O. Rasmussen, Lawrence Berkeley Laboratory Report No. LBL-19519, 1985.
[4] A. Goodman, Nucl. Phys. **A256**, 113 (1976).
[5] P. Ring, R. Beck, and H. J. Mang, Z. Phys. **231**, 10 (1970).
[6] T. L. Edigo and P. Ring, Nucl. Phys. **A388**, 19 (1980).
[7] J. Y. Zeng and T. S. Cheng, Nucl. Phys. **A405**, 1 (1983).
[8] J. Y. Zeng, T. S. Cheng, L. Cheng, and C. S. Wu, Nucl. Phys. **A411**, 49 (1983); **A414**, 253 (1984); **A421**, 125 (1984).
[9] C. S. Wu and J. Y. Zeng, Phys. Rev. C **39**, 666 (1989).
[10] I. Hamamoto, Nucl. Phys. **A271**, 15 (1976).
[11] R. Bengtsson and H. B. Håkansson, Nucl. Phys. **A357**, 61 (1981).
[12] P. Ring and P. Schuck, *The Nuclear Many-Body Problems* (Springer-Verlag, New York, 1980).
[13] D. J. Rowe, *Nuclear Collective Motion* (Methuen, London, 1970), p. 194.